Design and Expression of Organophosphorus Acid Anhydride Hydrolase Activity in Human Butyrylcholinesterase†

Charles B. Millard,*,‡ Oksana Lockridge,§ and Clarence A. Broomfield‡

United States Army Medical Research Institute of Chemical Defense, Aberdeen Proving Ground, Maryland 21010-5425, and Eppley Cancer Institute, University of Nebraska Medical Center, Omaha, Nebraska 68198-6805

Received July 6, 1995; Revised Manuscript Received September 25, 1995⊗

ABSTRACT: Serine esterases and proteases are rapidly and irreversibly inhibited by organophosphorus (OP) nerve agents. To overcome this limitation, we selected several residues that were predicted to be within 3−10 Å of both the active site Ser O^{γ} and the oxyanion hole of human butyrylcholinesterase for mutation to His (G115H, G117H, Q119H, and G121H). In remarkable contrast with wild-type (WT) and all other His mutants tested, G117H underwent spontaneous reactivation following OP inhibition to regain 100% of original esterase activity with maximum k_3 values of approximately 6.8×10^{-5} and 16×10^{-5} s^{-1} for GB (sarin) and VX, respectively, in 0.1 M Bis-Tris, 25 °C. The free energy of activation for k_3 was 19 kcal mol^{-1}, and measurement of pH dependence suggested that reactivation resulted from an acidic group with pK_a 6.2. To evaluate further the importance of His in achieving this result, we changed the same Gly to Lys (G117K) and compared its substrate and inhibitor kinetics with those of G117H. Both mutants retained esterase activity with K_m values similar to those of WT for neutral ester hydrolysis, but G117K did not reactivate. Complete reactivation proves that G117H is not irreversibly inhibited but instead functions as a catalyst for OP hydrolysis. Dephosphonylation is the rate-limiting step, and G117H effects overall rate constant enhancements of approximately 100- and 2000-fold above the uncatalyzed hydrolysis of GB and VX, respectively, at pH 6.0, 25.0 °C. We conclude that an appropriately positioned imidazolium ion in the oxyanion hole catalyzes dephosphonylation and, thereby, confers a novel organophosphorus acid anhydride hydrolase activity upon butyrylcholinesterase.

Acetylcholinesterase (EC 3.1.1.7; AChE[1]) and butyrylcholinesterase (EC 3.1.1.8; BuChE) arise from distinct genes but share key features of protein structure, and both efficiently catalyze acetylcholine hydrolysis [reviewed in Chatonnet and Lockridge (1989) and Taylor and Radic (1994)]. Catalysis is believed to proceed through displacement of the choline moiety by a nucleophilic serinyl oxygen atom to form an acyl-enzyme intermediate, followed by attack of an internal water molecule to deacylate and regenerate the enzyme (Wilson, 1951; Taylor & Radic, 1994). Like "B-type" proteases (Hess, 1971; Fastrez & Fersht, 1973), the esteratic chemistry is carried out by a triad of Ser, His, and an acidic residue. Presumably as a consequence of their preferred binding of the carbonyl transition-state tetrahedron (Pauling, 1946), serine proteases and esterases are susceptible to very fast inhibition by a wide array of transition-state analogs (Pauling, 1946; Lienhard, 1973). Inhibitors of this type include the organophosphorus (OP) anticholinesterases which are among the most toxic compounds ever made by man and are stockpiled as chemical warfare agents [reviewed in Taylor (1991) and Millard and Broomfield (1995)].

Although nerve agents are archetypical irreversible enzyme inhibitors (Dixon & Webb, 1979), spontaneous reactivation occurs on a limited basis for some OP−enzyme complexes [reviewed in Aldridge and Reiner (1972)]. Rational design of reactivation, therefore, is feasible. Complete sequencing of human BuChE (Lockridge et al., 1987) and atomic coordinates for *Torpedo californica* AChE (Sussman et al., 1991) enabled us to model BuChE and to identify several locations near the active site Ser198(*200*)[2] where a newly introduced histidinyl side chain might be positioned to catalyze spontaneous enzyme dephosphylation.[3] Human BuChE was chosen over AChE because comparative substrate specificities and molecular models both predict that it has a more open active site (Radic et al., 1993; Millard & Broomfield, 1992). We report here that one mutant, BuChE G117H, is an active cholinesterase that also catalyzes hydrolysis of the OP nerve agents GB (sarin) and VX.

† The opinions or assertions contained herein belong to the authors and should not be construed as the official views of the U.S. Army or the Department of Defense. This work was presented in abstract form at the 1995 Annual Meeting of the American Society for Biochemistry and Molecular Biology in San Francisco, CA. A patent application (U.S. No. 08/446,100) for design and creation of OPAAH activity in cholinesterase was submitted by the authors on behalf of the U.S. Government on May 20, 1995.

‡ U.S. Army Medical Research Institute of Chemical Defense.

§ University of Nebraska Medical Center.

⊗ Abstract published in *Advance ACS Abstracts,* November 15, 1995.

[1] Abbreviations: AChE, acetylcholinesterase (EC 3.1.1.7); AU, absorbance units; Bis-Tris, [bis(2-hydroxyethyl)amino]tris(hydroxymethyl)methane; BuChE, butyrylcholinesterase (EC 3.1.1.8); BuSCh, butyrylthiocholine; GB, isopropyl methylphosphonofluoridate (sarin); OP, organophosphorus anticholinesterase agents; OPAAH, organophosphorus acid anhydride hydrolase; p-NPA, *p*-nitrophenyl acetate; SE, standard error; VX, *O*-ethyl *S*-[2-[bis(1-methylethyl)amino]ethyl]-methylphosphonothiolate; WT, wild type (unmutated human butyrylcholinesterase).

[2] By convention, the italicized number in parentheses immediately following a BuChE amino acid residue refers to the corresponding amino acid residue in *T. californica* AChE. For example, BuChE S198(*200*) corresponds to AChE S200.

[3] The term "phosphylated" denotes phosphorylation and phosphonylation reactions without distinction (Hudson & Keay, 1960).

0006-2960/95/0434-15925$09.00/0

MATERIALS AND METHODS

Molecular Models. Computer-based models of human BuChE were constructed from the solved structure of AChE (Sussman et al., 1991) as described (Millard & Broomfield, 1992). Models of mutants also were made with the Biopolymer software of Insight II (version 2.3.5), and the lowest energy rotamers for substituted side chains were selected using the Insight II Discover (version 94.0) module (Biosym Technologies, San Diego, CA). All residues selected for replacement were modeled to be within 3−10 Å of both the active site Ser and the oxyanion hole (Table 1). Inhibitor structures were built with Biopolymer and energetically minimized with a full Newton−Raphson algorithm (Discover version 94). All modeling software was run on a Crimson 4D using the Irix operating system (Silicon Graphics, Mountain View, CA).

Site-Directed Mutagenesis. Four His mutants were made at Gly115(*117*), Gly117(*119*), Gln119(*121*), and Gly121-(*123*); a Lys mutant also was made at Gly117(*119*). We started with wild-type (WT) BuChE cloned in M13mp19 (McTiernan et al., 1987) and changed codons for each mutant by phosphorothioate site-directed mutagenesis (Nakamaye & Eckstein, 1986) using appropriate oligonucleotides that were synthesized from base−phosphoramidite precursors and purified by high-performance liquid chromatography. To confirm that no unwanted mutations had occurred, each resultant gene was sequenced entirely using a modification (Halloran et al., 1993) of the dideoxy terminator method (Sanger et al., 1977) and an automated DNA sequencer (Applied Biosystems, Foster City, CA).

Expression in Vitro. After cloning into a modified commercial shuttle vector and a cytomegalovirus promoter-driven expression vector (InVitrogen, San Diego, CA), BuChE genes were transfected stably into chinese hamster ovary (CHO-K) cells essentially as described (Masson et al., 1993). Enzyme expression was verified by measurement of catalyzed benzoylcholine hydrolysis (Kalow & Lindsay, 1955). Secreted BuChE was collected into serum-free medium.

Substrate Kinetics. Kinetic constants were determined by measuring the change in absorbance (ΔAU) at 405 nm of WT or mutant enzyme solutions using butyrylthiocholine (BuSCh; Sigma, St. Louis, MO) and 5,5′-dithiobis(2-nitrobenzoic acid) in 0.067 M Na/K phosphate buffer, pH 7.5, 25.0 °C (Ellman et al., 1961), or at 400 nm with *p*-nitrophenyl acetate (p-NPA; Sigma, St. Louis) containing less than 4% v/v acetonitrile, pH 8.0, 25.0 °C (Horton et al., 1978). At least two separate enzyme preparations were used, and substrate concentration ranges (Table 2) were chosen to observe "activation" of charged ester hydrolysis (Eriksson & Augustinsson, 1979; Cauet et al., 1987; Masson et al., 1993).

Inhibitor Kinetics. Isopropyl methylphosphonofluoridate (GB; also called "sarin") and *O*-ethyl *S*-[2-[bis(1-methylethyl)amino]ethyl]methylphosphonothiolate (VX) were obtained from the Edgewood Research, Development, and Engineering Center, Aberdeen Proving Ground, MD, and determined by gas chromatography to be >98% pure. Sarin and VX were chosen to typify nerve agents of the "G-type" and "V-type", respectively. Inhibitor structures are given in Table 3; greater than 75% of the VX is positively charged during enzyme inhibition based upon the pK_a of the tertiary nitrogen (Tammelin, 1957). Both GB and VX are extremely toxic and were handled according to established regulations governing chemical warfare surety materials.

Progressive inhibition studies at multiple inhibitor concentrations were done in 0.067 M Na/K phosphate buffer, pH 7.5, 25.0 °C. Residual activity was measured using a standard BuSCh activity assay of 1 mM BuSCh for WT or G117H and 8 mM BuSCh for G117K. Measurement of apparent I_{50} values established inhibitor concentration ranges (Table 3) that would give the shortest possible incubation times (0.5−10 min) to minimize error from spontaneous reactivation (Reiner & Aldridge, 1967).

Spontaneous Reactivation. For determination of the apparent spontaneous reactivation rate (k_{obs}), enzyme was inhibited 95% or greater. Excess inhibitor was removed by gel filtration under centrifugal force for 3 min at 4 °C (Penefsky, 1979) with disposable G-25 columns (Quick Spin G-25, Sephadex, fine; Boehringer Mannheim, Indianapolis, IN) that had been preequilibrated with >10 volume changes of 0.1 M Bis-Tris at specific pH values between 5.5 and 7.4 (±0.05; 25.0 °C) or with 0.067 M Na/K phosphate buffer, pH 7.5. In separate studies, to determine if either buffer catalyzed reactivation, G-25 columns were equilibrated at fixed pH values using several different buffer concentrations: 0.05, 0.10, and 0.50 M Bis-Tris (pH 7.1, 25 °C) or 0.067, 0.14, and 0.35 M Na/K phosphate (pH 7.5, 25 °C).

Column eluate (enzyme) was placed immediately in a 25.0 °C water bath. Samples were withdrawn at successive time points and added to the standard BuSCh activity assay to measure recovery of enzyme activity.

The "% reactivation" values for gel filtration experiments were determined by comparison of enzyme activity with that of control column eluates where the enzyme was mixed with buffer instead of inhibitor but otherwise treated identically.

Activation Energy of Spontaneous Reactivation. Temperature dependence of reactivation for G117H was measured in 0.067 M Na/K phosphate buffer, pH 7.5, at 22.0, 24.0, 26.0, 28.0, or 30.0 °C. Values of k_{obs} at each temperature were determined in triplicate with the standard BuSCh activity assay.

Measurement of VX Hydrolysis during Reactivation. In some experiments, either WT (0.3 unit/mL) or G117H (0.1 unit/mL) was inhibited 95% or greater with 800 μM VX, and immediately following the removal of excess inhibitor by gel filtration, an additional amount of VX (final concentration of 1 μM) was added to the column eluate. Small volumes (10 μL) subsequently were removed in triplicate at 10 min intervals and either (1) assayed for esterase activity with 1 mM BuSCh or (2) assayed for VX with 2 units of eel AChE (Sigma Chemical, St. Louis, MO) and acetylthiocholine by the method of Hammond and Forster (1989). The purpose of adding 1 μM VX to the inhibited G117H following gel filtration was to determine whether G117H reactivation resulted from dissociation of intact VX or from OP hydrolysis. Hydrolysis should have decreased the levels of intact VX during the reactivation phase. The assay for intact VX is based on the observation that VX reacts rapidly and stoichiometrically with eel AChE to inactivate the enzyme.

In separate controls, G117H was not inhibited with VX before gel filtration and received buffer instead of the second VX treatment. By mixing 10 μL from these control tubes with eel AChE and comparing the activity to that of the experimental samples, we were able to optimize the amount of eel AChE used such that the background hydrolysis of

Table 1: Human BuChE Mutants Designed To Possess OPAAH Activity

histidine mutant	estimated distances (Å): from His to active site Ser[a]	from His to "oxyanion hole"[b]	esterase activity?[c]	OPAAH activity?
G115H	5.9, 6.1	3.4, 6.2	no	no
G117H	6.7, 7.5	5.3, 2.4	yes	yes
Q119H	9.6, 8.5	7.8, 5.8	yes	no
G121H	8.9, 8.2	4.0, 6.2	no	no

[a] Obtained from models of human BuChE (Millard & Broomfield, 1992) based upon the structure of AChE (2.8 Å resolution; Sussman et al., 1991) by substituting with His and calculating the side-chain rotamer with the lowest energy. Distances are atomic center-to-center straight lines from the active site S198(*200*) O^{γ} to the imidazole N^{δ} and N^{ϵ} atoms, respectively, of the newly introduced His residue. [b] Distances are a straight line from the C^{β} atom of the newly introduced His residue to the polypeptide backbone nitrogen atoms of residues 116(*118*) and 117(*119*), respectively. Residues 116 and 117 are invariably Gly in WT cholinesterases and are believed to form part of the oxyanion hole. [c] Esterase activity was assayed with both butyrylthiocholine and benzoylcholine.

acetylthiocholine catalyzed by reactivated G117H did not interfere with the assay.

Statistical Analyses. Substrate kinetic constants were obtained by fitting velocity (ΔAU/dt) directly to nonlinear equations using an enzyme kinetic model fitting program (E-Z Fit, version 2.0; Perella, 1988). The SE values were determined by nonlinear regression using stepwise application of Nelder–Mead Simplex and Levenberg–Marquadt–Nash minimization of sum of the squares of the residuals [assumes a Gaussian distribution of error; reviewed in Johnson (1994)].

RESULTS

Preliminary experiments showed that Q119H and G117H retained the ability to catalyze the hydrolysis of both BuSCh and benzoylcholine but only G117H possessed organophosphorus acid anhydride hydrolase (OPAAH) activity (Table 1). On the basis of these results, we made G117K and compared its substrate and inhibitor kinetics with those of G117H and WT.

Substrate Kinetics. Hydrolysis of the neutral ester, p-NPA, followed Henri–Michaelis–Menten kinetics for WT, G117K, and G117H. The K_m values for p-NPA were similar for WT (6.1 mM) and both G117 mutants (12.5 mM).

BuSCh hydrolysis showed two K_m values depending upon the concentration range employed (Table 2). This was consistent with previous reports of BuChE "substrate activation" (Eriksson & Augustinsson, 1979), and therefore, we employed a model that considers the formation of two discrete binary complexes (ES and SE) and one ternary complex (SES; Aldridge & Reiner, 1972; Radic et al., 1993) (see Scheme 1). Assuming the simplest case where S binds equally well with E and ES ($K_s = K_{ss}$), enzyme velocities (v) were fit directly to the modified Haldane equation of Radic et al. (1993):

$$v = \left(\frac{1 + b[S]/K_{ss}}{1 + [S]/K_{ss}}\right)\left(\frac{V_{max}}{1 + K_m/[S]}\right) \quad (1)$$

BuSCh hydrolysis was well described by eq 1 for all three enzymes across a 5000-fold range of substrate concentrations (Figure 1). This enabled us to measure substrate activation of G117K which was not apparent below 10 mM BuSCh.

Table 2: Comparison of Substrate Kinetics for G117H and G117K

BuChE	substrate, S	[S] (mM)	K_m (mM)	lit.[a] K_m (mM)
	Data Fit to Henri–Michaelis–Menten Equation			
WT	p-NPA	1.0–10.0	6 ± 1	6.01
G117H	p-NPA	1.0–10.0	13 ± 2	
G117K	p-NPA	1.0–10.0	13 ± 2	
WT	BuSCh	0.01–0.11	0.016 ± 0.001	0.023
G117H	BuSCh	0.01–0.11	0.070 ± 0.003	
WT	BuSCh	1.25–6.25	0.20 ± 0.02	0.260
G117H	BuSCh	1.25–6.25	0.23 ± 0.02	
G117K	BuSCh	0.05–10.0	3.4 ± 0.2	

BuChE	[BuSCh] (mM)	K_m (mM)	K_{ss} (mM)	b value
	Data Fit to Modified Haldane Equation (Radic et al., 1993)[b]			
WT	0.006–25	0.025 ± 0.006	0.9 ± 0.1	3.1 ± 0.4
G117H	0.006–30	0.05 ± 0.01	0.8 ± 0.1	2.7 ± 0.3
G117K	0.006–100	0.40 ± 0.06	44 ± 5	4.0 ± 0.2

[a] The p-NPA value was determined with purified human serum BuChE at pH 6.9, 25.0 °C, by Horton et al. (1978); BuSCh literature values were measured with CHO-K cell WT BuChE at pH 7.5, 25 °C, by Masson et al. (1993). [b] Fitting to eq 1 was performed to account for the substrate activation phase observed with cationic BuSCh (see text for details).

Scheme 1[a]

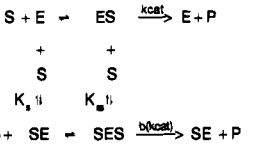

[a] E is BuChE; S is BuSCh; P is product; ES is the productive complex; SES is the ternary complex; K_{ss} is the substrate activation constant for BuChE; b is a weighting factor for k_{cat} that has been used to compare the efficiency of hydrolysis of SES relative to ES (Radic et al., 1993).

Scheme 2[a]

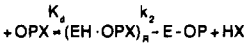

[a] EH is enzyme; OPX is an OP anticholinesterase inhibitor with leaving group X; $(EH{\cdot}OPX)_R$ is the reversible complex; E–OP is the phosphorylated, inactive enzyme; k_2 is the phosphorylation rate constant; K_d is a Michaelis-type constant governing formation of $(EH{\cdot}OPX)_R$ (Aldridge, 1950; Main & Iverson, 1966; Main, 1979).

Inhibition Constants. Inhibition of cholinesterase by OPs has been described as shown in Scheme 2. By formal analogy with the Henri–Michaelis–Menten equation for substrate steady state, Main (1964) postulated that if a reversible $(EH{\cdot}OPX)_R$ complex is formed, then

$$\rho = \frac{\ln(v_0/v_t)}{t} = \frac{k_2}{1 + K_d/i} \quad (2)$$

where k_2 and K_d are from Scheme 2, ρ is the observed first-order inhibition rate, v_0 is initial substrate hydrolysis velocity (ΔAU/min), v_t is velocity at some time, t, following addition of inhibitor, and i is the inhibitor concentration.

Our results supported this model. Moreover, the unusual resistance of G117H and G117K to OP inhibition allowed us to obtain evidence for formation of the reversible complex predicted by Main (1964) because plots of ρ as a function of inhibitor concentration were square hyperbolas. Nonlinear curve fits to eq 2 across a range of inhibitor concentrations resulted in the values of K_d and k_2 for G117H and G117K (Table 3).

The WT phosphylation rates (k_2) with GB and VX were too fast to measure by conventional kinetic methods, but

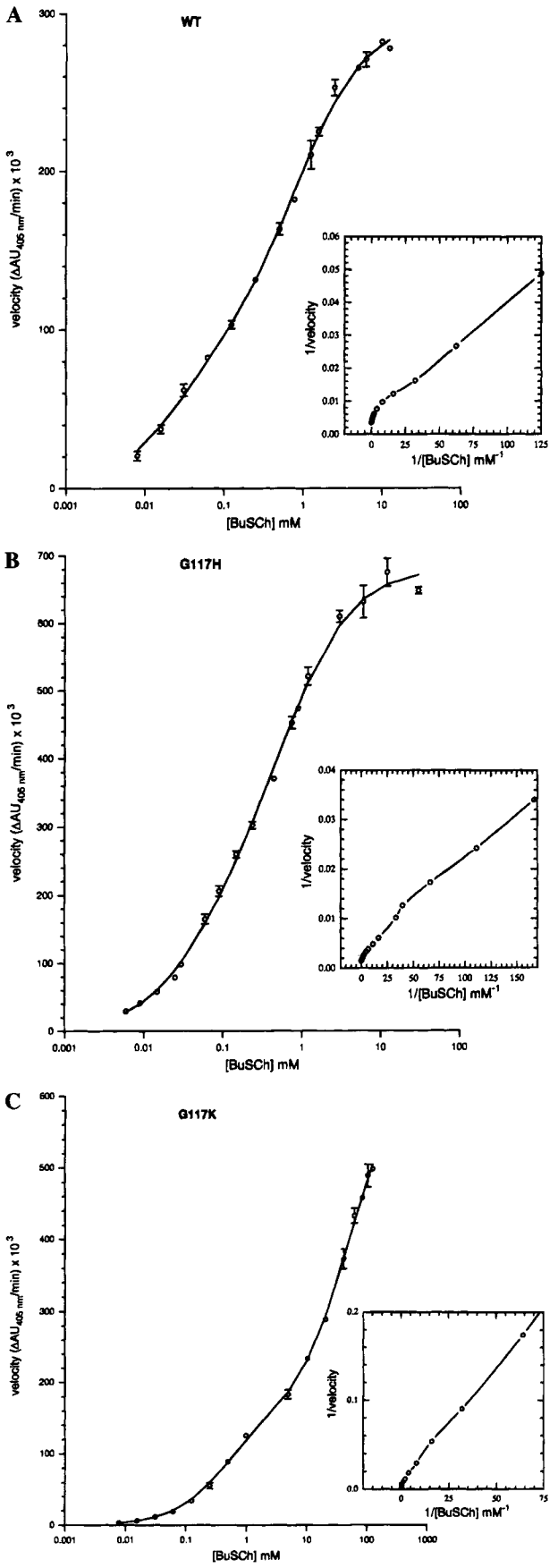

FIGURE 1: Concentration dependence for catalyzed hydrolysis of BuSCh. WT (panel A), G117H (panel B), and G117K (panel C) all show substrate activation. Each point represents the mean ± SD (some error bars are smaller than points) of three to five separate determinations, and curves shown are the nonlinear regression fits of raw velocity (ΔAU/min) data to eq 1 (constants from these fits are in Table 2). Insets are the curved double reciprocal plots.

lower limits (Table 3) were estimated from double reciprocal plots (Main, 1979).

Bimolecular rate constants (k_i) for G117H and G117K were calculated from K_d and k_2 using eq 3 (Main, 1979). The k_i for WT was determined as described (Cohen & Oosterbaan, 1963).

$$k_i = k_2/k_d \tag{3}$$

Using k_i as an estimation of the overall potency of the nerve agent, G117K and G117H showed approximately 6-fold and 7900-fold resistance, respectively, to GB inhibition compared to WT (Table 3). Both mutants showed 500–1000 times resistance to VX inhibition. The large decrease in k_i for G117K with VX relative to GB was caused primarily by a 23-fold increase in K_d (Table 3).

We estimated the relative affinities of several cholinesterases for the two related OP inhibitors, GB and VX, from the dimensionless ratio of the measured or reported K_d values (Adams & Whittaker, 1950; Creighton, 1984; Radic et al., 1993):

$$\Delta(\Delta G^\circ)_{VX-GB} = RT \ln(K_d^{VX}/K_d^{GB}) \tag{4}$$

where T is 298.2 K and R is the gas constant [1.987 cal/(mol·K)]. The positive $\Delta(\Delta G^\circ)_{VX-GB}$ value obtained for G117K suggested that, unlike other cholinesterases including G117H (Table 4), the Lys mutant forms a much less stable $(EH{\cdot}OPX)_R$ complex with VX than it does with GB.

Analysis of Reactivation. Spontaneous cholinesterase reactivation has been described as shown in Scheme 3.

Following removal of excess inhibitor by gel filtration, only G117H underwent spontaneous reactivation (Figure 2). Reactivation was apparently first order for at least 3×10^3 s, and therefore, data were fit to the equation:

$$\ln\left(\frac{v_\infty - v_t}{v_\infty - v_i}\right) = -k_{obs}t + c \tag{5}$$

where k_{obs} is the observed reactivation rate constant, v denotes substrate hydrolysis velocity (ΔAU/min), v_i is the inhibited velocity before removal of excess inhibitor, v_t is velocity at time t (zero time was defined as entry of the enzyme–inhibitor mix into the G-25 column), and v_∞ is the final velocity achieved after maximum reactivation.

Phosphylated cholinesterases may undergo an "aging" reaction that results in formation of a phosphonate ester monoanion and irreversible enzyme inhibition (Hobbiger, 1955; Berends et al., 1959). Aging is caused by fission of the alkoxy O–R bond of the phosphonate fragment, where R is the ethyl and isopropyl group for VX and sarin, respectively. Because reactivation and aging behave as two competing first-order reactions, the true reactivation rate constant, k_3, can be calculated at the end of the reaction (Hovanec et al., 1977):

$$k_3 = (\%\ \text{react})(k_{obs})/100 \tag{6}$$

where k_{obs} is defined in eq 5, k_3 is from Scheme 3, and "% react" is the final percent reactivation achieved.

Reactivation of inhibited G117H after gel filtration proceeded to between 90% and 110% of control. Furthermore, G117H underwent 100% reactivation in inhibition experiments without gel filtration. From these observations

Table 3: Comparison of Inhibition Constants[a]

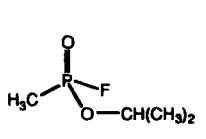

GB (sarin)

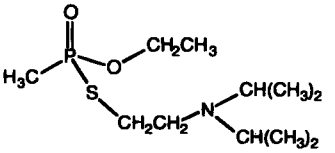

VX

BuChE	[GB] (μM)	n	$K_d \pm$ SE (μM)	$k_2 \pm$ SE ($\times 10^4$ s^{-1})	k_i (M^{-1} s^{-1})[b]
WT	0.05–0.13	3		>1000[c]	22000 ± 4000
G117H	1.25–200	9	110 ± 10	3.0 ± 0.2	2.7 (2.4–3.4)
G117K	1.6–50	12	13 ± 2	440 ± 20	3400 (800–3500)
BuChE	**[VX] (μM)**	**n**	**$K_d \pm$ SE (μM)**	**$k_2 \pm$ SE ($\times 10^4$ s^{-1})**	**k_i (M^{-1} s^{-1})[b]**
WT	0.05–0.13	3		>1000[c]	30400 ± 2800
G117H	40–150	16	50 ± 9	12.6 ± 0.9	25 (20–35)
G117K	20–101	13	300 ± 100	150 ± 40	50 (30–100)

[a] Experiments were performed in 0.067 M Na/K phosphate buffer, pH 7.5, 25 °C (see text for details); n is the number of inhibitor concentrations used. [b] Calculated for G117K and G117H as k_2/K_d with ranges in parentheses from Marquadt–Nash nonlinear fits to eq 2. For the WT, k_i values were estimated by the method of Cohen and Oosterbaan (1963) and are expressed as mean ± SE of three separate determinations. For comparison, the k_i of human serum BuChE has been reported as 23 333 M^{-1} s^{-1} (Heilbronn-Wikstrom, 1965) and 35 000 M^{-1} s^{-1} (Skrijaric-Spoljar & Simeon, 1993) for GB and VX, respectively. [c] The lower limit of k_2 for WT was estimated by the method of Main (1964).

Table 4: Relative Stability of Cholinesterase–OP Complexes

	K_d (μM)	k_2 (s^{-1})	$\Delta(\Delta G°)_{VX-GB}$[b] (kcal)
GB			
eel AChE[a]	2.2	1.05	
rabbit brain AChE[a]	1.7	0.42	
BuChE G117H	110	0.0003	
BuChE G117K	13	0.044	
VX			
eel AChE[a]	1.7	0.92	−0.2
rabbit brain AChE[a]	0.9	0.51	−0.4
BuChE G117H	50	0.0013	−0.5
BuChE G117K	300	0.015	+1.9

[a] Inhibition constants for AChE were determined using stopped-flow methodology with p-NPA substrate at pH 7.5 and 0.067 M phosphate buffer, 25.0 °C, by Gray and Dawson (1987). [b] Calculated for the values of K_d from eq 4.

Scheme 3[a]

$$\text{E-OP} \xrightarrow[H_2O]{k_3} \text{E-OH} + \text{PO}^- + \text{H}^+$$

[a] E–OP is the phosphorylated enzyme (from Scheme 2); PO^- is the hydrolyzed inhibitor; E–OH is the reactivated enzyme (Main, 1979).

and eq 6, we conclude that k_{obs} approximates k_3 from Scheme 3 for G117H inhibited with GB or VX.

pH Dependence. Plots of k_3 for G117H reactivation as a function of pH in 0.1 M Bis-Tris at 25.0 °C were sigmoidal with slower rates at higher pH (Figure 3). To estimate the pK_a inflection point (Dixon, 1953), we used a modified four-parameter logistic fit:

$$(k_3)_H = \frac{k_{max} - k_{min}}{1 + e^{b(pH-c)}} + k_{min} \quad (7)$$

where b is the slope constant, k_{max} and k_{min} are the upper and lower asymptotes of the curve, respectively, and c is the inflection point that corresponds to the pK_a for the acid(s) upon which spontaneous reactivation depends. Fitting k_3 at each pH to $(k_3)_H$ of eq 7 resulted in pK_a values of approximately 6.2 for both inhibitors with $k_{3(max)}$ values of 6.8×10^{-5} s^{-1} and 16×10^{-5} s^{-1} for GB and VX, respectively.

Comparison of k_3 values at pH 7.5, 25 °C, showed that G117H reactivation was consistently faster in 0.067 M Na/K phosphate buffer than in 0.1 M Bis-Tris buffer following inhibition with both GB and VX (cf. Figures 2 and 3 at pH 7.5). This was not due to the buffer catalyzing dephosphonylation, however, because k_3 was not increased by raising the concentrations of either Bis-Tris or Na/K phosphate buffer.

OPAAH Activity. Prolonged stability of VX in CHO cell medium (control without BuChE) at 25.0 °C enabled us to measure its hydrolysis during G117H reactivation. Fresh addition of 1 μM VX following gel filtration delayed but did not prevent the spontaneous reactivation of G117H. The observed rate of VX loss in the presence of G117H, as measured by eel AChE activity (Hammond & Forster, 1989), was consistent with the measured k_3 value of approximately 10^{-4} s^{-1} in 0.067 M Na/K phosphate buffer, pH 7.5, 25.0 °C (Figure 2B). Reactivation of G117H resulted in complete hydrolysis of VX (i.e., eel AChE activity in tubes spiked with reactivation mixture was 100% of control). Separate control experiments showed that inhibited WT did not affect the stability of VX in the eel AChE assay.

For reactivation of G117H, the free energy of activation (E_a) was determined by the Arrhenius equation:

$$\ln k_3 = -\frac{E_a}{RT} + c \quad (8)$$

Plots of ln k_3 as a function of $1/T$ were linear with slopes of $-E_a/R$. The E_a value was 19 ± 3 kcal/mol (mean ± SD of three determinations) for G117H inhibited by GB.

DISCUSSION

Effects of Disrupting the Oxyanion Hole. The amide backbone hydrogens at Gly116(*118*) and Gly117(*119*) are believed to be strong hydrogen bond donors within the BuChE oxyanion hole that stabilize the carbonyl oxygen atoms of the substrate transition state, as well as the phosphonyl oxygen of OP inhibitors (Sussman et al., 1991; Qian & Kovach, 1993; Masson et al., 1994). Both G117H and G117K catalyze ester hydrolysis and are phosphonylated by OPs, suggesting that the BuChE oxyanion hole has the capacity to complement substrate or inhibitor transition states despite the presence of bulky side chains. Changes in kinetic

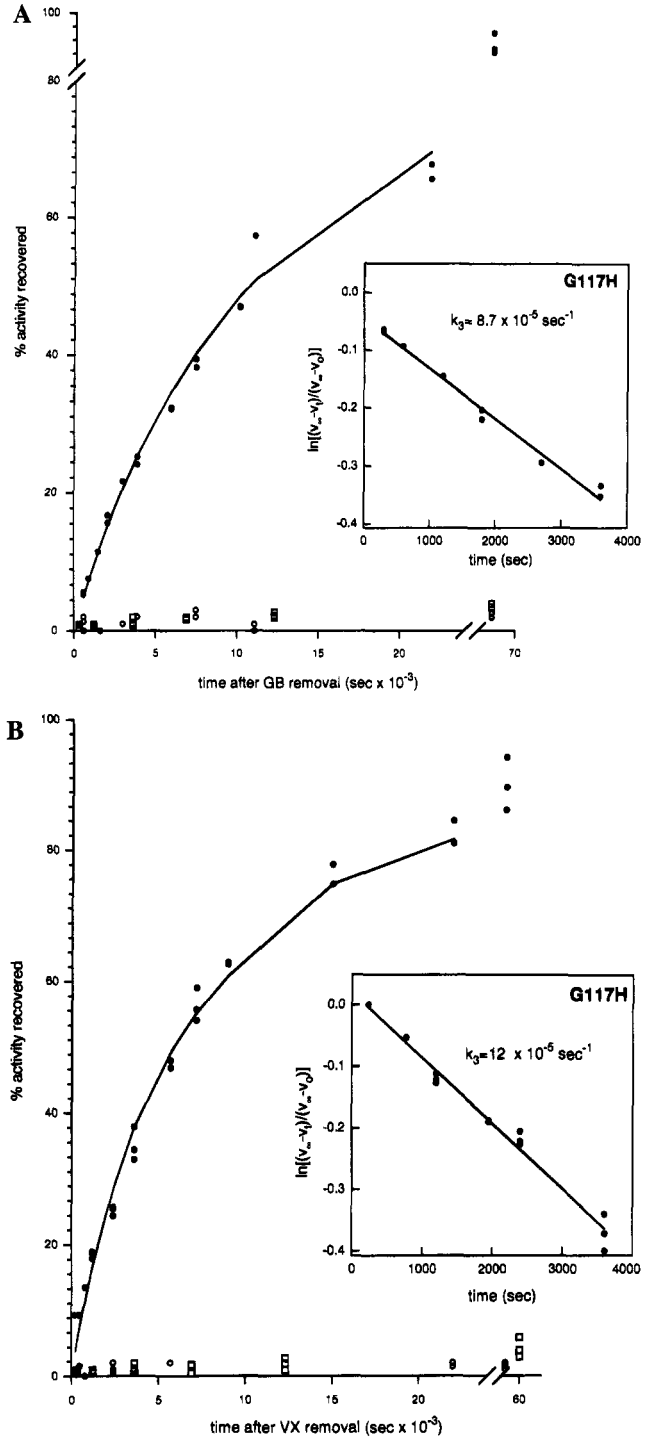

FIGURE 2: Representative spontaneous reactivation of G117H (closed circles) following inhibition with GB (panel A) or VX (panel B). Experiments shown were conducted in 0.067 M Na/K phosphate buffer, pH 7.5, 25 °C. Insets show that reactivation can be treated as first order for at least 3 × 10^3 s. The rates are from eq 5. Using the same methodology, WT BuChE (open circles) and G117K (open squares) exhibited comparatively insignificant reactivation.

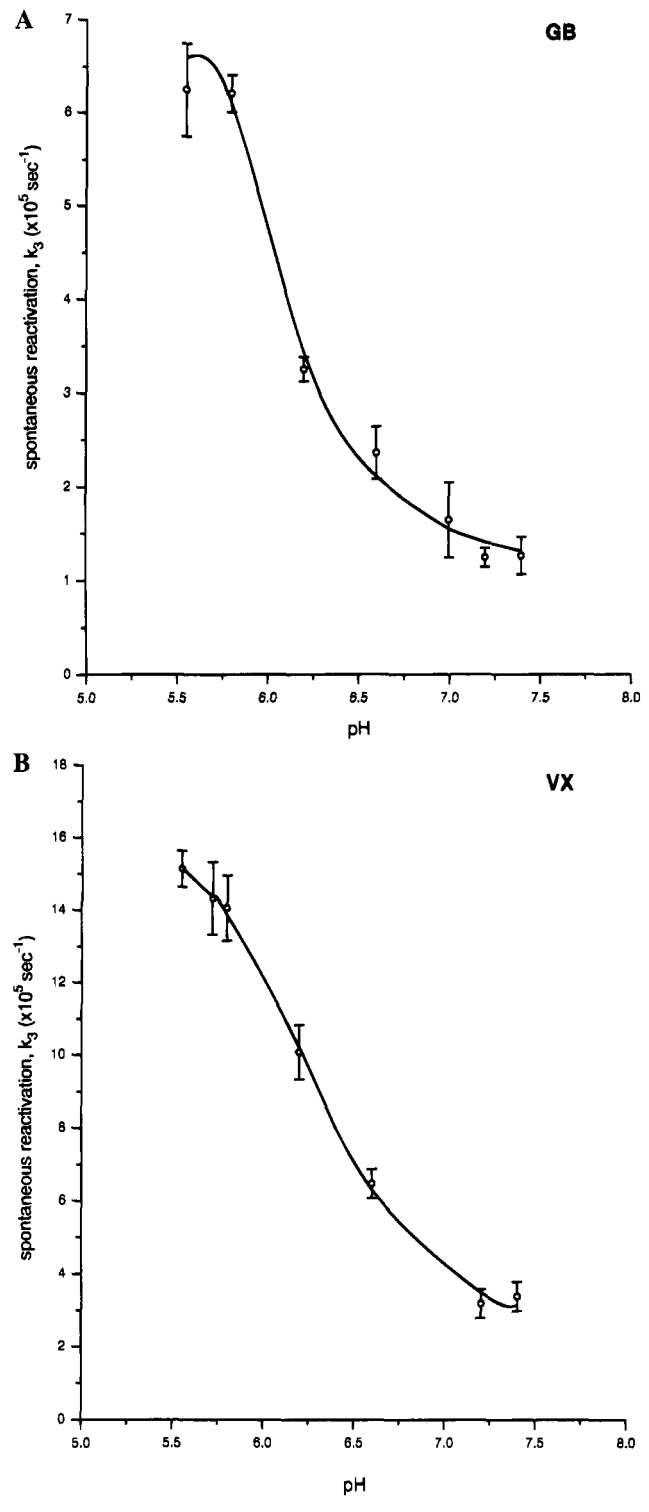

FIGURE 3: Spontaneous reactivation of BuChE G117H acid catalyzed following phosphonylation with either GB (panel A) or VX (panel B). Each point represents the mean ± SD of three to five experimental determinations of the G117H spontaneous reactivation rate (k_3) in 0.1 M Bis-Tris at the indicated pH, 25.0 °C. Curves shown are fits of the data to eq 7, the pH at maximum rate of change is approximately 6.2 for both inhibitors, and the $k_{3(max)}$ (upper asymptote) values are 6.8 × 10^{-5} and 16 × 10^{-5} s^{-1} for GB and VX, respectively. Note that k_3 for both inhibitors is significantly elevated in phosphate buffer at pH 7.5 compared to Bis-Tris (cf. Figure 2).

constants show, however, that natural complementation has been disturbed by both mutations.

Weakening of the reversible complexes for G117K with cations is evidenced by examination of three different constants: (1) a 16- and 8-fold elevation in the G117K K_m for BuSCh compared to WT and G117H, respectively, but little effect on the K_m for p-NPA (Table 2), (2) an approximately 50-fold increase in K_{ss} for G117K compared to WT or G117H (Table 2), and (3) an approximately 23-fold increase in K_d for G117K with VX compared to GB (Table 3). The comparatively large, positive $\Delta(\Delta G°)_{VX-GB}$ value for G117K also supports the deduction that binding of VX to the Lys mutant is uncharacteristically weak (Table 4).

Energy-minimized molecular models predict that Lys117 protrudes up into the active site gorge toward D70(*72*)

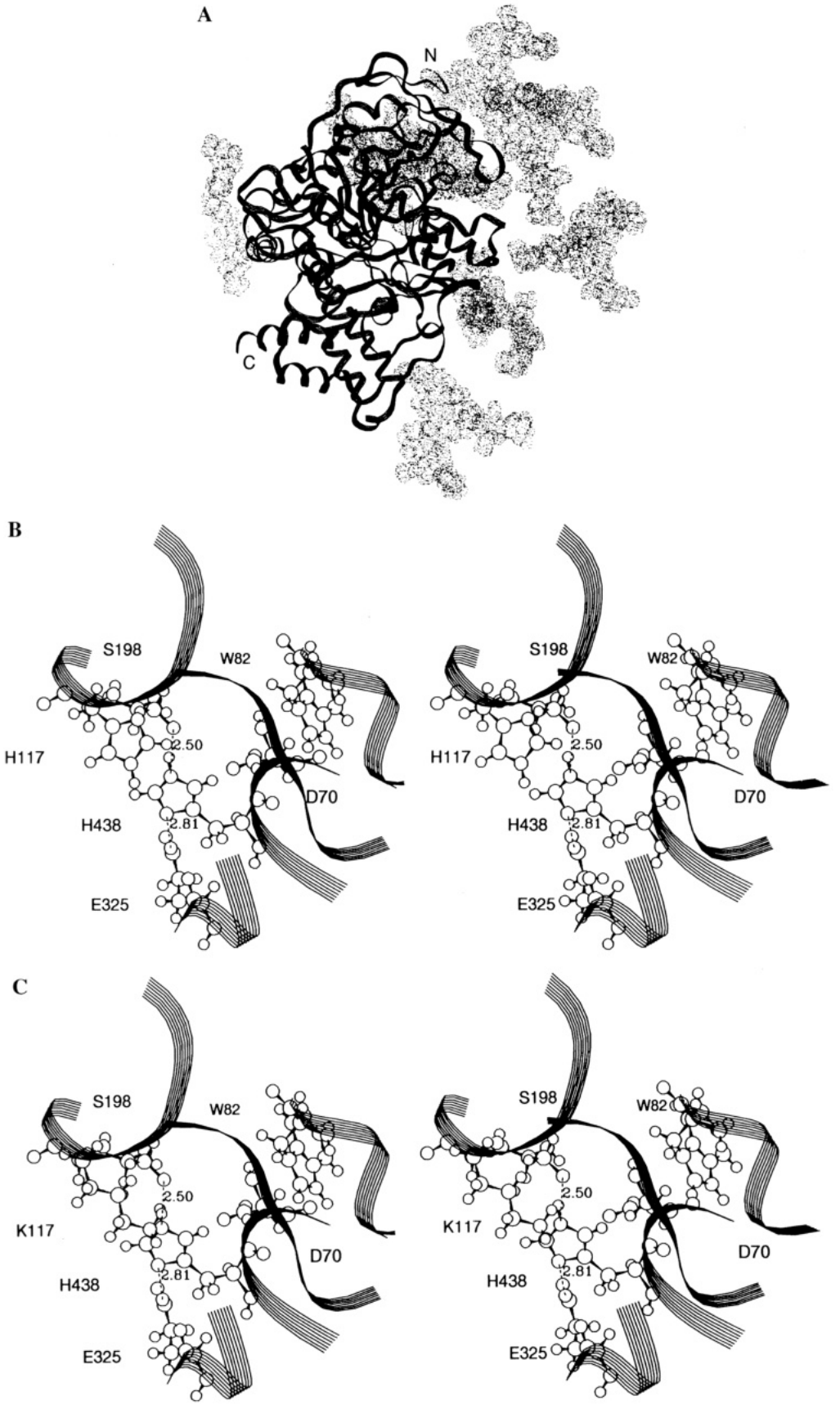

FIGURE 4: Energy-minimized model of the glycosylated, human BuChE monomer viewed down the putative "gorge" leading to the active site (N is the amino terminus and C is the carboxy terminus). Dots represent the putative van der Waals radii surface of N-linked oligosaccharides (panel A). Panels B and C are stereo images with the protein in precisely the same orientation as panel A to show close-up views of the the mutated residues G117H and G117K, respectively. Broken lines denote the charge relay system of the active site (modeled distances of 2.5 Å from S198 O^{γ} to H438 N^{ϵ} and 2.8 Å from H438 N^{δ} to E325 O^{ϵ}). Note that K117 (panel C) protrudes up into the active site gorge (out of the page) toward the presumed "anionic site" at D70. Modeled distances from K117 N^{ζ} to D70 O^{δ} and to D70 O^{ϵ} are only 5.5 and 5.6 Å, respectively. The geometry of the imidazole, in contrast, confines H117 more squarely in the oxyanion hole (8.0 Å from H117 N^{ϵ} to D70 O^{δ}). From these models, the K117 N^{ζ} atom could hinder access of cationic ligands to S198 and the final trimethyl binding site (Hasan et al., 1981) at W82.

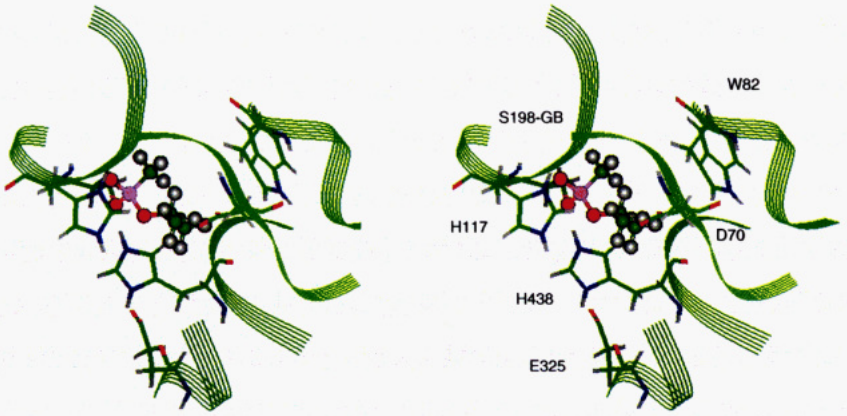

FIGURE 5: Energy-minimized stereo model of GB phosphonylated G117H at pH 5.8 (same orientation as in Figure 4B). BuChE modeled from AChE and the absolute P(*R*) configuration of GB were the starting structures. After presumed stereochemical inversion during phosphonylation, the resultant GB fragment (solid ball and stick) is shown in the P(*S*) configuration with the phosphonyl oxygen atom in the oxyanion hole (3.0 and 2.2 Å to the backbone nitrogen atoms of Gly116(*118*) and His117, respectively). From this model, a hydrogen on the N^{δ} atom of His117 in the oxyanion hole is close (3.8 Å) to the phosphonyl oxygen atom while the N^{ϵ} of His438 is within hydrogen-bonding distance (2.6 Å) of the active site S198 O^{γ} (solid red ball).

(Figure 4). From such a position, the positively charged K117 N^{ζ} atom could destabilize binding of the ionized nitrogen atoms of BuSCh and VX either by direct charge−charge repulsion or by neutralizing the Coulombic effects of D70. The presence of a negative charge at D70 is important for the efficient binding of positively charged substrates and inhibitors (McGuire et al., 1989; Neville et al., 1990). For example, the D70G variant shows a 21-fold reduction in VX binding compared to WT BuChE but no difference in binding to GB or other neutral OP inhibitors (Skrijaric-Spoljar & Simeon, 1993).

Phosphonylation rate constants (k_2) for both mutants are decreased significantly compared to WT (Table 3). Slower phosphonylation rates are clearly undesirable in converting cholinesterases to OPAAH enzymes but may be useful for creating transgenic animals (e.g., beneficial insects) that are resistant to OP poisons.

OPAAH Activity. Inhibited G117H, but not G117K, WT, or the other oxyanion hole His mutants tested, undergoes spontaneous reactivation to 100% esterase activity. We reject the possibility that transfected cells produce a contaminating OPAAH activity because reactivation was detected in all transfections with the gene for G117H using both CHO-K and human 293 cells, whereas transfection with genes for the other mutants or WT did not result in OPAAH activity. The alternative possibility of noncovalent inhibition of G117H was rejected because VX was completely degraded during reactivation. If G117H reactivation reflected the slow reversal of a noncovalent inhibitor−His117 complex, then levels of intact VX should have increased during E−I dissociation.

The E_a for G117H reactivation (19 ± 3 kcal mol^{-1}) compares favorably with dephosphorylation of eel AChE following inhibition with diisopropyl fluorophosphate (20.1 kcal mol^{-1}; Lanks & Seleznick, 1981), as well as that of rat BuChE following inhibition with diethyl *p*-nitrophenol phosphate (14.4 kcal mol^{-1}; Davison, 1953).

The overall rate-limiting step for the OPAA hydrolytic activity of G117H apparently is k_3 (10^{-5}−10^{-4} s^{-1}). The uncatalyzed rate constants for GB and VX hydrolysis are 6 × 10^{-7} s^{-1} and 8 × 10^{-8} s^{-1}, respectively (pH 6.0, 25 °C; Beach & Sass, 1961; Epstein et al., 1974). If the rate-limiting k_3 approximates the G117H OPAA hydrolytic k_{cat}, then the new enzyme activity enhances the hydrolysis rate constants by approximately 100- and 2000-fold for GB and VX, respectively, at pH 6.0.

Phosphotriesterases and previously characterized OPAA hydrolases generally do not catalyze VX hydrolysis. However, an apparent k_{cat} of 56 s^{-1} was measured for the phosphotriesterase from *Pseudomonas diminuta* by monitoring GB hydrolysis in the presence of enzyme (Dumas et al., 1990). This is much faster than G117H, but direct comparison may be misleading because of pH and metal ion effects on the hydrolysis of GB. The hydrolysis rate constant for GB increases by orders of magnitude if the pH drops below 5−6 (Beach & Sass, 1961). The GB hydrolysis rate also is increased as much as 100-fold by the presence of metal ions such as Mg^{2+} or Cu^{2+} (Epstein & Rosenblatt, 1958), and the *P. diminuta* phosphotriesterase is a metalloenzyme. There are no confounding effects of metal ion or pH changes upon OP stability in our determination of G117H rate constants because we measured the return of esterase activity following removal of excess inhibitor.

Mechanism of OPAAH Activity. Natural cholinesterases employ a general base mechanism to catalyze several different reactions including deacylation, decarbamylation, and the limited dephosphylation reported for AChE [reviewed in Aldridge & Reiner (1972)]. These reactions all show bell-shaped pH dependence curves with rates that increase from pH 5.5 to pH 7.5 (Reiner & Aldridge, 1967; Main, 1979; Järv, 1984). The opposite is observed for k_3 of G117H (Figure 3), leading us to disfavor the possibility that His117 is acting as a general base [cf. Järv (1984)].

Chymotrypsin and thrombin inhibited with GB also undergo acid-catalyzed spontaneous reactivation. The maximum k_3 for both proteases is 1.9 × 10^{-6} s^{-1} at pH 5.1, 25 °C (Green & Nicholls, 1959). This is about 40-fold slower than G117H, and the proteases regain less than 50% of their original activity (Green & Nicholls, 1959; Thompson, 1970). In view of the results obtained with BuChE, however, it may be possible to enhance serine protease reactivation generally by introduction of a His in the oxyanion hole.

On the basis of the crystal structure of diethyl phosphorylated chymotrypsin (Harel et al., 1991), several groups have modeled inhibited cholinesterases with the active site His438-(*440*) imidazolium ion close enough to hydrogen bond with the alkoxy oxygen atom of the phosphonate fragment during enzyme aging (Qian & Kovach, 1993; Segall et al., 1993;

Masson et al., 1994). This is consistent with the observation that aging is an acid-catalyzed reaction that depends upon a group of pK_a 6.3 (presumably the active site His; Michel et al., 1967). Kovach (1988) forecasts that the electron density of the phosphorus and, hence, the strength of the His438–alkoxy hydrogen bond should be inversely proportional to the spontaneous reactivation rate. From its location in the oxyanion hole (Figure 5), the protonated N^{δ} of His117 could disrupt this critical hydrogen bond by withdrawing electrons from the phosphonyl oxygen. This also would free the His438 imidazolium to hydrogen bond with the Ser198 O^{γ}, thereby further weakening the P–O^{γ} bond and enabling G117H to reactivate instead of aging. Proof of mechanism and enhancement of G117H activity await structural data and subsequent treatment of each enzyme–inhibitor complex as a unique, stereospecific phosphoester.

Rational design of substrate specificity around existing active site chemistry is increasingly feasible (Bone et al., 1989; Radic et al., 1993), but disruption of natural complementation remains a primary barrier to engineering enzymes with new functions [cf. Jackson et al. (1994)]. The modest new OPAAH activity of BuChE G117H can be viewed as turning to advantage the fact that the inhibitors are already "hemisubstrates" which were optimized as chemical warfare agents to mimic the substrate transition state.

REFERENCES

Adams, D. H., & Whittaker, V. P. (1950) *Biochim. Biophys. Acta 4*, 543–558.

Aldridge, W. N. (1950) *Biochem. J. 46*, 451–460.

Aldridge, W. N., & Reiner, E. (1972) in *Enzyme Inhibitors as Substrates. Interaction of Esterases with Esters of Organophosphorus and Carbamic Acids*, Chapter 4, pp 53–91, North-Holland, Amsterdam.

Beach, L. K., & Sass, S. (1961) *Anal. Chem. 33*, 901–906.

Berends, F., Posthumus, C. H., Sluys, I. V. D., & Deierkauf, F. A. (1959) *Biochim. Biophys. Acta 34*, 576–578.

Bone, R., Silen, J. L., & Agard, D. A. (1989) *Nature 339*, 191–195.

Cauet, G., Friboulet, A., & Thomas, D. (1987) *Biochem. Cell Biol. 65*, 529–535.

Chatonnet, A., & Lockridge, O. (1989) *Biochem. J. 260*, 625–634.

Cohen, J. A., & Oosterbaan, R. A. (1963) in *Handbuch der experimentellen pharmakologie* (Koelle, G. B., Ed.) Chapter 7, pp 299–373, Springer-Verlag, Berlin.

Creighton, T. E. (1984) in *Proteins: Structures and Molecular Principles*, pp 336–339, Freeman & Co., New York.

Davison, A. N. (1953) *Biochem. J. 54*, 583–590.

Dixon, M. (1953) *Biochem. J. 55*, 161–170.

Dixon, M., & Webb, E. C. (1979) in *Enzymes* (Boyer, P. D., Ed.) 3rd ed., Chapter VIII, p 333, Academic Press, New York.

Dumas, D. P., Durst, H. D., Landis, W. G., Raushel, F. M., & Wild, J. R. (1990) *Arch. Biochem. Biophys. 277*, 155–159.

Ellman, G. L., Courtney, K. D., Andres, V., Jr., & Featherstone, R. M. (1961) *Biochem. Pharmacol. 7*, 88–95.

Epstein, J., Callahan, J. J., & Bauer, V. E. (1974) *Phosphorus 4*, 157–163.

Epstein, J., & Rosenblatt, D. H. (1958) *J. Am. Chem. Soc. 80*, 3596–3598.

Eriksson, H., & Augustinsson, K.-B. (1979) *Biochim. Biophys. Acta 567*, 161–173.

Fastrez, J., & Fersht, A. R. (1973) *Biochemistry 12*, 2025–2034.

Gray, P. J., & Dawson, R. M. (1987) *Toxicol. Appl. Pharmacol. 91*, 140–144.

Green, A. L., & Nicholls, J. D. (1959) *Biochem. J. 72*, 70–75.

Halloran, N., Du, Z., & Wilson, R. K. (1993) *Methods Mol. Biol. 23*, 297–315.

Hammond, P. S., & Forster, J. S. (1989) *Anal. Biochem. 180*, 380–383.

Harel, M., Su, C.-T., Frolow, F., Ashani, Y., Silman, I., & Sussman, J. L. (1991) *J. Mol. Biol. 221*, 909–918.

Hasan, F. B., Elkind, J. L., Cohen, S. G., & Cohen, J. B. (1981) *J. Biol. Chem. 256*, 7781–7785.

Heilbronn-Wikstrom, E. (1965) *Sven. Kem. Tidskr. 77*, 598–630.

Hess, G. P. (1971) in *The Enzymes* (Boyer, P. D., Ed.) Vol. 3, pp 213–248, Academic Press, New York.

Hobbiger, F. (1955) *Br. J. Pharmacol. 10*, 356–362.

Horton, G. L., Lieske, C. N., & Lowe, J. R. (1978) *Pestic. Sci. 9*, 135–138.

Hovanec, J. W., Broomfield, C. A., Steinberg, G. M., Lanks, K. W., & Lieske, C. N. (1977) *Biochim. Biophys. Acta 483*, 312–319.

Hudson, R. F., & Keay, L. (1960) *J. Chem. Soc.* 1859.

Jackson, D. Y., Burnier, J., Quan, C., Stanley, M., Tom, J., & Wells, J. A. (1994) *Science 266*, 243–247.

Järv, J. (1984) *Bioorg. Chem. 12*, 259–278.

Johnson, M. (1994) *Methods Enzymol. 240*, 1–22.

Kalow, W., & Lindsay, H. A. (1955) *Can. J. Biochem. Physiol. 33*, 568–574.

Kovach, I. M. (1988) *J. Enzyme Inhib. 2*, 199–208.

Lanks, K. W., & Seleznick, M. J. (1981) *Biochim. Biophys. Acta 660*, 91–95.

Lienhard, G. E. (1973) *Science 180*, 149–154.

Lockridge, O., Bartels, C. F., Vaughan, T. A., Wong, C. K., Norton, S. E., & Johnson, L. L. (1987) *J. Biol. Chem. 262*, 549–557.

Main, A. R. (1964) *Science 144*, 992–993.

Main, A. R., & Iverson, F. (1966) *Biochem. J. 100*, 525–531.

Main, A. R. (1979) *Pharmacol. Ther. 6*, 579–628.

Masson, P., Adkins, S., Gouet, P., & Lockridge, O. (1993) *J. Biol. Chem. 268*, 14329–14341.

Masson, P., Gouet, P., & Clery, C. (1994) *J. Mol. Biol. 238*, 466–478.

McGuire, M. C., Nogueira, C. P., Bartels, C. F., Lightstone, H., Hajra, A., Van Der Spek, A. F. L., Lockridge, O., & LaDu, B. N. (1989) *Proc. Natl. Acad. Sci. U.S.A. 86*, 953–957.

McTiernan, C., Adkins, S., Chatonnet, A., Vaughan, T. A., Bartels, C. F., Kott, M., Rosenberry, T. L., LaDu, B. N., & Lockridge, O. (1987) *Proc. Natl. Acad. Sci. U.S.A. 84*, 6682–6686.

Michel, H. O., Hackley, B. E., Jr., Berkowitz, L., List, G., Hackley, E. B., Gillilan, W., & Pankau, M. (1967) *Arch. Biochem. Biophys. 121*, 29–34.

Millard, C. B., & Broomfield, C. A. (1992) *Biochem. Biophys. Res. Commun. 189*, 1280–1286.

Millard, C. B., & Broomfield, C. A. (1995) *J. Neurochem. 64*, 1909–1918.

Nakamaye, K. L., & Eckstein, F. (1986) *Nucleic Acids Res. 14*, 9679–9698.

Neville, L. F., Gnatt, A., Padan, R., Seidman, S., & Soreq, H. (1990) *J. Biol. Chem. 265*, 20735–20738.

Pauling, L. (1946) *Chem. Eng. News 24*, 1375–1377.

Penefsky, H. S. (1979) *Methods Enzymol. 56*, 527–530.

Perella, F. W. (1988) *Anal. Biochem. 174*, 437–447.

Qian, N., & Kovach, I. M. (1993) *FEBS Lett. 336*, 263–266.

Radic, Z., Pickering, N. F., Vellom, D. C., Camp, S., & Taylor, P. (1993) *Biochemistry 32*, 12074–12084.

Reiner, E., & Aldridge, W. N. (1967) *Biochem. J. 105*, 171–179.

Sanger, F., Nicklen, S., & Coulson, A. R. (1977) *Proc. Natl. Acad. Sci. U.S.A. 74*, 5463–5467.

Segall, Y., Waysbort, D., Barak, D., Ariel, N., Doctor, B. P., Grunwald, J., & Ashani, Y. (1993) *Biochemistry 32*, 13441–13450.

Skrijaric-Spoljar, M., & Simeon, V. (1993) *J. Enzyme Inhib. 7*, 169–174.

Sussman, J. L., Harel, M., Frolow, F., Oefner, C., Goldman, A., Toker, L., & Silman, I. (1991) *Science 253*, 872–879.

Tammelin, L. E. (1957) *Acta Chem. Scand. 11*, 1340–1349.

Taylor, P. (1991) in *The Pharmacological Basis of Therapeutics* (Gilman, A. G., Nies, A. S., Rall, T. W., & Taylor, P., Eds.) pp 131–150, Macmillan, New York.

Taylor, P., & Radic, Z. (1994) *Annu. Rev. Pharmacol. Toxicol. 34*, 281–320.

Thompson, A. R. (1970) *Biochim. Biophys. Acta 198*, 392–395.

Wilson, I. B. (1951) *Biochim. Biophys. Acta 7*, 520–525.

BI951530O